

PAPER • OPEN ACCESS

## Simulation of partial discharges in cavities and streamers with high spatial resolution

To cite this article: D I Karpov *et al* 2017 *J. Phys.: Conf. Ser.* **899** 082001

View the [article online](#) for updates and enhancements.

### Related content

- [Streamers and partial discharges in water](#)  
S M Korobeynikov and A V Melekhov
- [Automized Recognition of Partial Discharges in Cavities](#)  
Edward Gulski, Peter H. F. Morshuis and Frederik H. Kreuger
- ["Relay-race" mechanism of propagation of partial discharges in condensed dielectrics at linearly increasing voltage](#)  
A L Kupershtokh and D I Karpov

# Simulation of partial discharges in cavities and streamers with high spatial resolution

D I Karpov<sup>1</sup>, A L Kupershtokh<sup>1</sup>, M B Meredova<sup>1</sup> and M V Zuev<sup>1</sup>

<sup>1</sup> Lavrentyev Institute of Hydrodynamics SB RAS, 15 Lavrentyev Prosp., Novosibirsk, 630090, Russia

E-mail: [karpov@hydro.nsc.ru](mailto:karpov@hydro.nsc.ru)

**Abstract.** The electrical characteristics of partial discharges in cavities and streamer channels were simulated with the high spatial and temporal resolution. The parallel computations on graphic processing units were applied for the numerical solution of this system of equation. The current in an external circuit as well as the true charge during partial discharge were calculated for different positions of a single void and for two voids in electrode gap. The parallel algorithm for the stochastic growth of streamer in a dielectric was developed. The electric characteristics of the partial discharges due to the streamer growth were studied.

## 1. Introduction

Registration of the partial discharges (PD) activity in dielectrics subjected to the action of the high voltages is a one of the modern and effective methods of estimation of the reliability of high voltage equipments. The electrical strength of the air and other gases is by the order of magnitude lower than that of the condensed dielectric therefore PD occurs in cracks and in voids in solid dielectrics and in bubbles in liquids usually. There are two main types of the PD known [1,2]. The first type includes microdischarges in small cavities which always exist both on the electrode surface and in the bulk of the dielectrics. The second one corresponds to the PDs inside the channels of branching structures (streamers) which grow in the bulk of the dielectrics or along the interface between two dielectrics.

To simulate the PDs of the first type, three models are known: the “equivalent circuit of capacitors”, the “dipole model”, and the model of the “complete calculation of the electric field inside the gap”. The method of an equivalent circuit is still used in practical estimations of the isolation performance which is based on the consideration of an electrotechnical circuit consisting of discrete capacitors [3]. The drawbacks of this model are obvious, and the “dipole model” was proposed. The polarization of a cavity due to PD can be described with the model of the electric dipole roughly [4,5]. The electric field of this dipole changes the distribution of charges on the electrodes and the distribution of the electric field inside the gap. The properties of these two models are thoroughly discussed in the review [6]. The third model known at present is the model of the complete calculation of the electric field inside the gap according to the Poisson’s equation which was realized qualitatively for the first time for a single cavity in solid dielectrics in [7]. The roles of the position of the cavity in an electrode gap and the size of the cavity in formation of the so called apparent  $Q_{app}$  and true charges  $Q_{true}$  of the PD were studied in [8]. The authors of this work used the static calculation of



electric fields before and after the PD in order to estimate the value of  $Q_{app}$  and  $Q_{true}$ . The conductive cavity was simulated with the high values of the dielectric permittivity  $\varepsilon$ .

The second type of the PD are the microdischarges inside the channels of branching structures (streamers), growing in the bulk of the dielectric or along the interface of two different dielectrics. The high electric field strength at the tip of the channels is provided by the transfer of electric charge along the channels from the electrode to the tips due to PDs that occur stochastically in different segments of the channels. The streamer development is accompanied by the flashes of light and the synchronous current pulses that are typical for the PD [9,10]. The model of the pulsed conductivity proposed in [11] allowed for the first time simulating this pulsed character of the currents. Most simulations with the models of stochastic growth of branching streamer structures [11-13] were performed on lattices with a rough spatial resolution because of the lack of the computational resources. In those simulations, the fine spatial structure of the streamer channels could not be represented with the real spatial resolution. Thus the electrical characteristics of the channels during the growth were described only qualitatively.

In the present work, we performed the simulation of the both types of the PDs in condensed dielectrics taking into account the dynamics of the electrical charges due to conductivity of the PD plasma. A computer programs were developed for parallel computations of these problems on very large spatial lattices. This allowed us simulating the PDs with very high resolutions in space and time.

## 2. The electrodynamic model

The electric field and the charge distribution in the gap between electrodes were calculated at each time step by solving the following system of equations. In the region occupied by dielectric

$$\text{div}(\varepsilon \nabla \varphi) = 0 . \quad (1)$$

In the conducting regions of the electrode gap

$$\text{div}(\varepsilon \nabla \varphi) = -4\pi\rho . \quad (2)$$

Here  $\varepsilon$  is the dielectric permittivity of a substance. For the conductive regions of the electrode gap (streamer channels or cavities) we used the equations

$$\frac{\partial \rho}{\partial t} = -\text{div} \mathbf{j} , \quad \mathbf{j} = \sigma \cdot \mathbf{E} , \quad \mathbf{E} = -\nabla \varphi . \quad (3)$$

Here  $\varphi$  and  $\mathbf{E}$  are the electric field potential and the electric strength, respectively,  $\rho$  is the electric charge density,  $\sigma$  is the average conductivity of plasma during PD,  $\mathbf{j}$  is the current density.

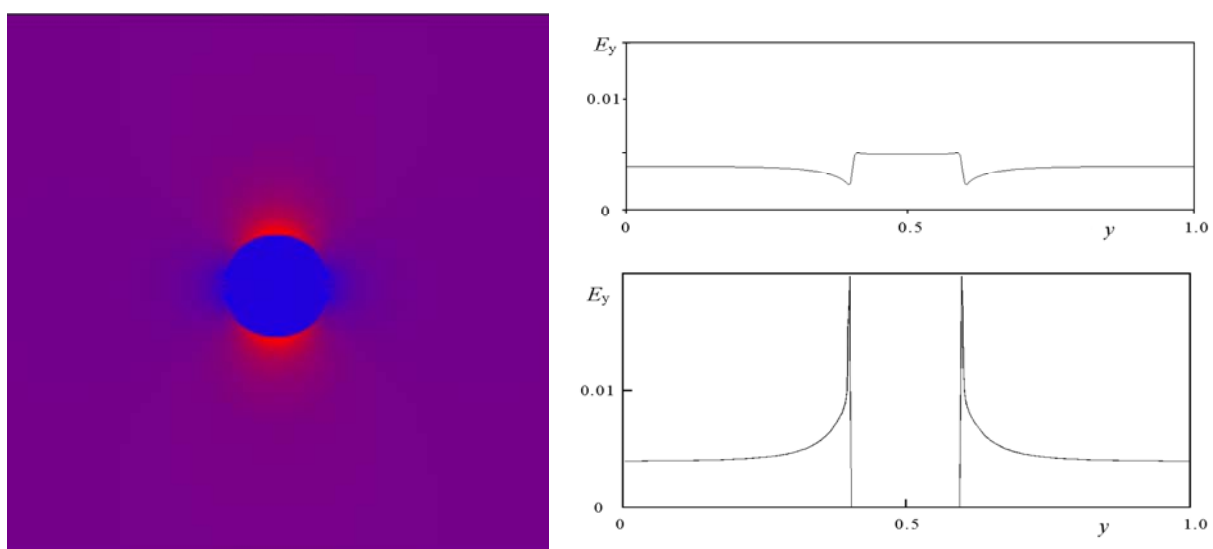


**Figure 1.** The field distribution  $E_y(x, y)$  after the PD (left) and the plots  $E_y(y)$  along symmetry axis before the PD (upper right) and after the PD (lower right) are shown. The lattice size is  $256 \times 256 \times 256$ .

The duration of one PD is of the order of nanosecond. We neglected the injection of the charges to the dielectrics from the void-dielectric interface and the diffusion of the charges in the dielectric media on the time scales of several tens of nanoseconds. The boundary conditions were  $\varphi = 1$  on the upper electrode and  $\varphi = 0$  on the lower one. The values of  $\varphi$  changed linearly on the side surfaces of the simulation region. The calculation of the electric field distribution takes more than 90 per cent of the simulation time that imposes the restriction on the size of the lattice.

### 3. Field calculations with Graphic Processing Units

The conservative implicit in time finite-difference numerical method [12] was realized on NVIDIA Graphic Processing Units (GPU) for calculating the currents and the electric potential from the system (1) – (3). At each time step, the distribution of the potential was calculated by simple iterations. The CUDA programming technology with C language was used to implement the algorithm on GPU. The graphic card with 512 processor cores was used. Each lattice node was handled in its own thread. The blocks of 32 threads provided the maximum computing performance. The use of GPU accelerated the calculations by about 100 times. All the data were allocated in the fast global memory of GPU.

### 4. Simulations of partial discharges in voids with rigid walls

Two and three-dimensional calculations of the PD in one and two voids were performed. The spherical void with the rigid walls with the dielectric permittivity  $\varepsilon = 1$  was placed at the different positions to the gap filled with the dielectric with  $\varepsilon = 2$ . In the first approximation, we did not take into account deformation of the bubble and the hydrodynamic processes related to the PD in it. The distribution of the vertical component of the electric field stress  $E_y$  in the central cross-section of the three-dimensional electrode gap is shown in figure 1 for the case of central positioning of one void as well as the plots of  $E_y$  along the symmetry axis before the PD and after the PD. The distances are reduced to the gap length  $d$ .

We used the Maxwellian relaxation time  $\tau = \varepsilon / 4\pi\sigma$  as the scale of time. The magnitudes of current (as well as charges) can be calculated for the specific values of the applied voltage, the gap length  $d$  and the conductivity in clear way. Nevertheless, only the relative values of the charges are of importance in this study. Figure 2 shows the electric current in the external circuit and the true electric charge in the single bubble for the two cases. The bubble was placed on the electrode surface such as its center was in the central point of the electrode in the first case. In the second case, the position of the bubble was in the center of the electrode gap. The radiuses of the bubbles were the same and were equal to  $R = 0.125d$ . The PD current was of the order of the magnitude higher for the first case than for the second one although the difference in the values of the true charges was only about 15 per cent. We imply that true charge is the charge of the same sign that is generated in voids during the PD.

The magnitudes of PD charges were studied if the discharges occurred simultaneously in two voids. The voids were placed symmetrically at the same distances of  $0.25d$  from the electrodes. The results of the simulations were compared with that for the single void of the same radius placed at the same distance of  $0.25d$  from one of the electrode. The figure 3 shows the plots of the reduced current in the external circuit and the true charge reduced in one void and in two voids. The true charge  $Q_{\text{true}}$  and the charge registered in the external circuit  $Q_{\text{app}}$  were calculated at the different positions of the single void and for the two voids (table 1). The true charge per one void is represented in the last column of the table. The true charge in a void does not change noticeably with the position of the void. Nevertheless, the charge flowing in the external circuit increases significantly when the distance from the void to the nearest electrode becomes smaller. For two voids, the true charge per one void is practically the same as for the case of one void, but the value of  $Q_{\text{app}}$  increases considerably with comparison to the case of the single void. Nevertheless, the PD current increases only by about 25 per cent in this case (figure 3).

### 5. The model of streamer growth

We used the stochastic model of streamer growth developed earlier in order to simulate the PD in a streamer. The streamer is simulated with the conducting segments connecting neighbor nodes of the lattice. New elements of the streamer appeared with some probability that is a function of the local electric field. The probabilities of the appearance of the new segments were calculated using the following algorithm. Let us start from a node that belongs to the streamer structure. Find the value of the projection of the electric field  $E_i$  onto each of the possible direction to the neighbor nodes that belong to the dielectric state. If the Field Fluctuation Criterion (FFC) [11]

$$E_i > E_* - \delta_i, \tag{4}$$

was fulfilled then the segment between these nodes became the new conducting element.

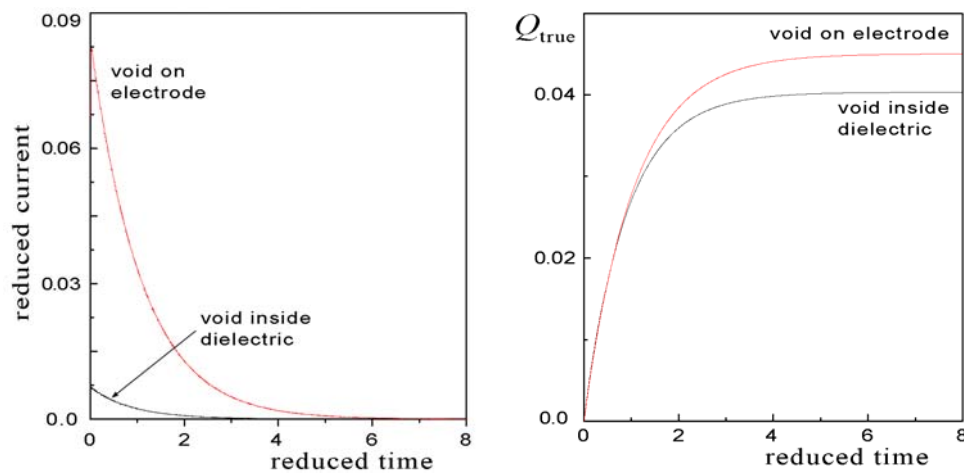


**Figure 2.** The electric current in a circuit (left) and the electric charge inside the cavity (right) for the positions of the single void on the electrode surface and in the center of the electrode gap.

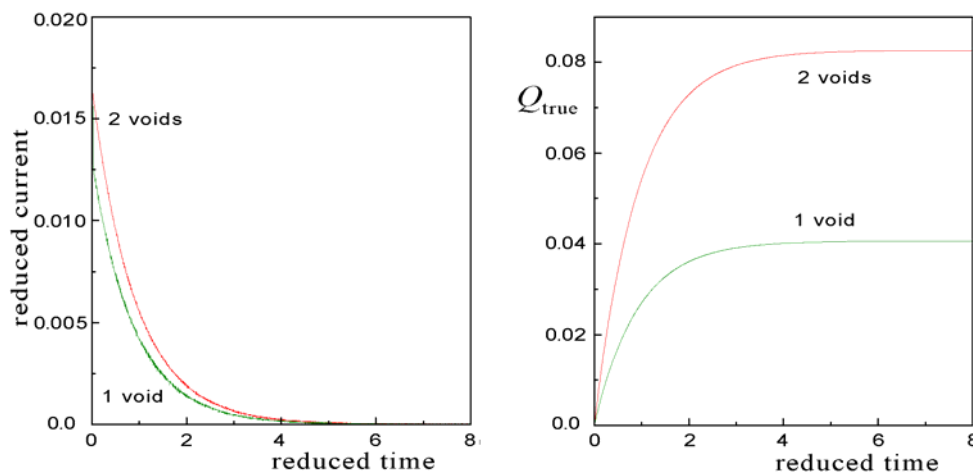


**Figure 3.** The electric current in a circuit (left) and the electric charge (right) in the two voids with comparison to the same characteristics for the single void.

**Table 1.** Calculated values of  $Q_{app}$  and  $Q_{true}$  at different position of the single void in the electrode gap and for the two symmetrically placed voids after single PD.

| Positions of the centers of the voids | $0.01 d$ | $0.25 d$ | $0.5 d$ | $0.25 d$ and $0.75 d$ |
|---------------------------------------|----------|----------|---------|-----------------------|
| $Q_{app}$                             | 0.0224   | 0.00292  | 0.00157 | 0.0038                |
| $Q_{true}$                            | 0.045    | 0.0406   | 0.0403  | 0.0413                |

The distribution  $\varphi(\delta) = \exp(-\delta/g)/g$  was used for the probabilities of the fluctuations  $\delta$  that was equivalent to the random variable  $\delta = -g \ln(\xi)$ . Here,  $\xi$  is a random value uniformly distributed within the interval from 0 to 1. The parameter was  $E_* = -g \cdot \ln(A \cdot \tau / h)$ , where  $h$  is the lattice step,  $\tau$  is the time step,  $A$  is the constant of the model related to the local velocity of streamer tip by

$$v(E) = A \cdot \exp(E/g). \quad (5)$$

Here  $g$  is the model parameter defining the rate of the velocity increase with the electric field stress.

### 6. The parallel algorithm for the growth of a branching streamer

The parallel algorithm was developed for the stochastic choice of the new segments of the streamer structure. The three-dimensional lattice was divided into the equal cubic blocks of sizes  $4 \times 4 \times 4$  lattice nodes. An indexing array  $B[i]$  was additionally used with number of elements  $N_{64} = N_x \times N_y \times N_z / 64$ . Here  $N_x$ ,  $N_y$ , and  $N_z$  are the sizes of the lattice. The zero value was assigned to the element  $B[i]$  if there is no streamer nodes within the  $i$ -th block. The value of the  $i$ -th element was set to 1 if there is at least one of the ends of the segment belonging to the streamer structure inside the block. The treatment of the array  $B[i]$  was carried out with the GPU. Each element was handled in one calculating thread. If  $B[i] = 0$  the treatment of this block was cancelled. If  $B[i] = 1$  the nodes of the lattice inside this block that belong to dielectric state were examined. If one of these nodes has a neighbor node that belongs to the streamer structure we checked if the FFC criterion (4) was fulfilled for these two nodes. If the condition (4) was true the dielectric node became the new site of streamer structure. The constant conductivity  $\sigma$  was assigned to this new segment.

### 7. PD current during initial stage of a streamer development

We simulated the streamer growth on the cubic lattice with the spatial spacing  $h = 2.5 \mu\text{m}$ . The calculations were performed on the lattice of the size of  $386 \times 386 \times 386$  nodes. We used the needle-plane electrode geometry with the needle tip radius of  $2.5 \mu\text{m}$  and the distance from the tip to the plane electrode of  $0.5 \text{ mm}$ . The coefficient of the field non-uniformity was 33. The time step was  $\tau = 10 \text{ ps}$ . The model parameters  $g = 0.7 \text{ MV/cm}$  and  $A = 1.4 \cdot 10^{-7} \text{ m/s}$  were obtained by the comparison of the simulations to the experimental data [14]. The dielectric permittivity was equal to 2 for the dielectric and 1 for plasma channel.

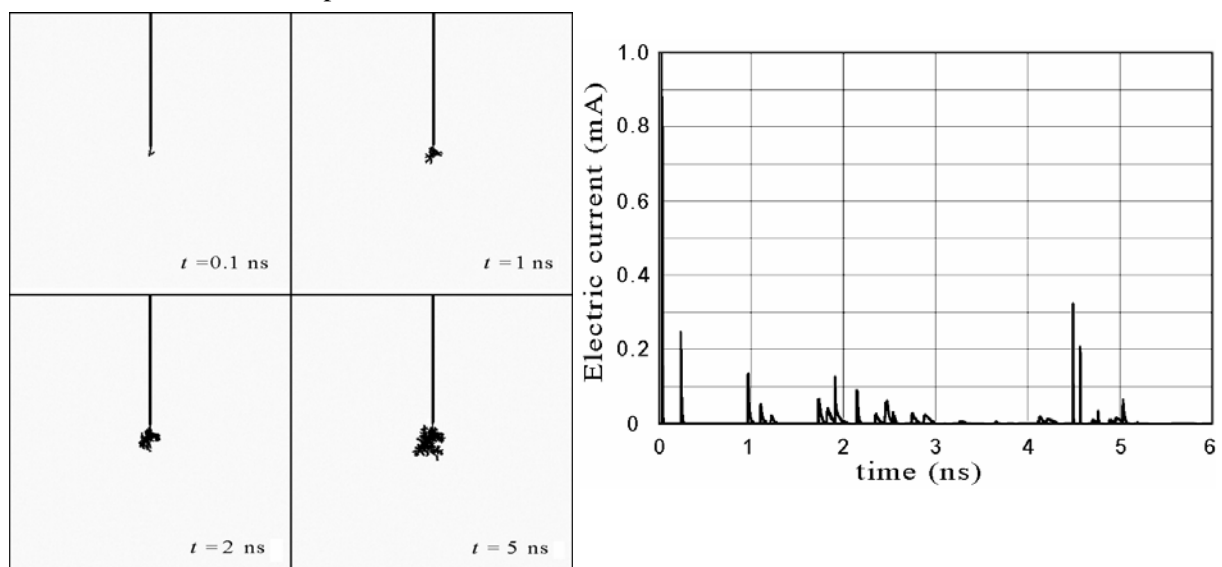


**Figure 4.** Initial stages of the growth of the streamer structure (left) and the pulses of the PD current accompanying the streamer growth in the external circuit.  $V = 30 \text{ kV}$ .

The figure 4 shows the four shots of the streamer structure at the initial stage of the growth. The growth is stepwise. When the electric field is high enough in some region of the dielectric the new segments of the streamer channels grow in this region. Then the streamer stops until the electric field stress before the channel tip reaches the value sufficient to the further growth due to charge relaxation in the channels. Each step of growth is accompanied by the current pulses of the magnitude that is significantly higher than the continuous component of the current during the stops. Figure 4 shows the PD current corresponding to the streamer growth. These magnitudes correspond to the value of the conductivity of the channels averaged across the section  $\sigma = 3.8$  S/m.

## 8. Conclusion

The simulations of the PDs in voids and in streamer channels in condensed dielectrics were performed with the use of parallel algorithms on GPU on large spatial lattices. Thus, the electrical characteristics of PDs were calculated more accurately than it was made before.

## Acknowledgments

The study was supported by the Russian Scientific Foundation (grant No. 16-19-10229).

## References

- [1] Kreuger F H, Gulski E and Krivda A 1993 Classification of partial discharges *IEEE Transactions on Electrical Insulation* **28**(6) 917–31
- [2] Niemeyer L 1995 A generalized approach to partial discharge modeling *IEEE Transactions on Dielectrics and Electrical Insulation* **2**(4) 510–28
- [3] Gemant A, Von Philipoff W 1932 Die Funkenstrecke mit Vorkondensator *Zeitschrift für Technische Physik* **13**(9) 425–30
- [4] Pedersen A 1986 Current pulses generated by discharges in voids in solid dielectrics. A field theoretical approach *IEEE Int. Symp. Electrical Insulation (IESI), 86CH2196-4-DEI*, pp 112.
- [5] Pedersen A, Crichton G C and McAllister I W 1995 The functional relation between partial discharges and induced charge *IEEE Transactions on Dielectrics and Electrical Insulations* **2** 535–43
- [6] Lemke E 2012 A critical review of partial-discharge models *IEEE Electrical Insulation Magazine* **28**(6) 11–6
- [7] Wu K, Suzuoki Y and Dissado L A 2004 The contribution of discharge area variation to partial discharge patterns in disk-voids *J. Phys. D: Appl. Phys.* **37**(13) 1815–23
- [8] Ovsyannikov A G and Korobeynikov S M 2016 "Apparent" and true charges of partial discharges *Proceedings of the 2016 IEEE International Conference on Dielectrics, ICD 2016, University of Montpellier: Montpellier, France.*
- [9] Ushakov V Ya, Klimkin V F, Korobeynikov S M Impulse breakdown of liquids. – Berlin: Springer-Verlag, 2007
- [10] Lesaint O, Saker A, Gournay P, Tobazéon R, Aubin J and Mailhot M 1998 Streamer propagation and breakdown under ac voltage in very large oil gaps *IEEE Transactions on Dielectrics and Electrical Insulations* **5**(3) 351–9.
- [11] Kupershtokh A L 1992 Fluctuation model of the breakdown of liquid dielectrics *Soviet Technical Physics Letters* **18**(10) 647–49
- [12] Karpov D I and Kupershtokh A L 1998 Models of streamers growth with "physical" time and fractal characteristics of streamer structure *Conference Record of the 1998 IEEE International Symposium on Electrical Insulation, IEEE No. 98CH36239 (Arlington, USA)* pp 607–10
- [13] Kupershtokh A L and Karpov D I 2006 Simulation of the development of branching streamer structures in dielectric liquids with pulsed conductivity of channels *Technical Physics Letters* **32**(5) 406–9
- [14] Lesaint O and Gournay P 1994 On the gaseous nature of positive filamentary streamers in hydrocarbon liquids. I and II *J. Phys D: Appl. Phys.* **27**(10) 2111–27